A&A 399, 441–448 (2003)
DOI: 10.1051/0004-6361:20021800

Astronomy & Astrophysics

H_0 measurement from VLT deep I–band surface brightness fluctuations in NGC 564 and NGC 7619⋆

S. Mei[1], M. Scodeggio[2], D. R. Silva[3], and P. J. Quinn[3]

[1] Institut d'Astrophysique Spatiale, Université Paris-Sud, Bât. 121, 91405 Orsay, France
[2] Istituto di Fisica Cosmica G. Occhialini, Via Bassini 15, 20133 Milano, Italy
[3] European Southern Observatory, Karl-Schwarzschild-Strasse 2, 85748 Garching, Germany

Received 28 June 2002 / Accepted 22 November 2002

Abstract. We have measured the Hubble constant H_0 in NGC 564 at $cz \approx 5800$ km s^{-1} and in NGC 7619 at $cz \approx 3700$ km s^{-1} with deep I–band Surface Brightness Fluctuation distance measurements at the ESO Very Large Telescope (VLT). We obtain $H_0 = 70 \pm 7 \pm 6$ km s^{-1}/Mpc for NGC 564 and $H_0 = 68 \pm 6 \pm 6$ for NGC 7619. The actual SBF sample used for the measurement of H_0 in the Hubble Space Telescope Key Project on the Extragalactic Distance Scale (Freedman et al. 2001) amounts to six galaxies. When we combine the measurements from this work with our previous VLT I–band SBF distance measurement in IC 4296 (Mei et al. 2000), we obtain: $H_0 = 68 \pm 5 \pm 6$ km s^{-1}/Mpc. When we add the Freedman et al. (2001) SBF sample, we obtain $H_0 = 71 \pm 4 \pm 6$ km s^{-1}/Mpc.

Key words. galaxies: distances and redshifts – cosmology: cosmological parameters

1. Introduction

Future Cosmic Microwave Background missions like MAP (`http://map.gsfc.nasa.gov/`) and Planck (`http://astro.estec.esa.nl/SA-general/Projects/Planck/`) promise to obtain definitive measurements of cosmological parameters, achieving an accuracy around 1%. Over the last few years, however, the accuracy of such measurements has improved considerably, as many efforts have been carried out to obtain accurate measurements for the Hubble constant H_0, to reduce the uncertainty in its determination from 50% to approximately 10%. The most important among these efforts has been the Hubble Space Telescope Key Project on the Extragalactic Distance Scale (HSTKP; Freedman et al. 2001 and references therein) where the value of H_0 was measured to be $H_0 = 72 \pm 8$ km s^{-1}, based on a coherent Cepheid calibration of four of the most dependable and precise methods for galaxy distance measurements: Tully–Fisher, Fundamental Plane, SNIa and Surface Brightness Fluctuations. Other important contributions were provided, among others, by Ajhar et al. (2001), Blakeslee et al. (2001), Jensen et al. (2001), Gibson & Stetson (2001), Liu & Graham (2001), Tonry et al. (2000), Suntzeff et al. (1999), Jha et al. (1999), Giovanelli et al. (1997), Hjorth & Tanvir (1997).

H_0 measurements are affected not only by uncertainties in the derivation of the cosmological distance ladder, but also by the presence of local deviations from the smooth Hubble flow. The average peculiar velocity for galaxies and clusters of galaxies are of the order of 100–300 km s^{-1} (Davis et al. 1997; Giovanelli et al. 1998; Dale et al. 1999). Therefore to minimise their effect on the determination of H_0, it is preferable to select target objects beyond 4000 km s^{-1}, where the peculiar motions amount to no more than ≈10%–15% of the total velocity. This requirement has led to a number of projects trying to build samples of redshift-independent distance estimates restricted to galaxies located beyond 4000–5000 km s^{-1} (Dale et al. 1999; Hudson et al. 2001; Colless et al. 2001; Jensen et al. 2001).

Among the methods used to obtain accurate galaxy distance estimates, Surface Brightness Fluctuations (SBF) are, at present, one of the most accurate and better physically understood methods available. The method was introduced by Tonry & Schneider (1988) (a recent review has been given by Blakeslee et al. 1999a) and is based on the very simple fact that the Poissonian distribution of unresolved stars in a galaxy produces fluctuations in each pixel of the galaxy image. The variance of these fluctuations is inversely proportional to the square of the galaxy distance. The SBF amplitude is defined to be precisely this variance, normalised to the mean flux of the galaxy in each pixel (Tonry & Schneider 1988).

The absolute magnitude of the fluctuation is not a constant, but depends on the age and metallicity of the stellar population within the galaxy. Tonry et al. (1997) and Tonry et al. (2001) have quantified these dependencies using an extensive sample of I and V band observations, which are used to empirically calibrate the dependence of the I–band fluctuation magnitude on $(V-I)$ colour. The absolute calibration is then obtained using a set of 5 galaxies with independent Cepheid distances.

As part of the HSTKP, Ferrarese et al. (2000a) have obtained their own calibration based on accurate Cepheid distances to six spiral galaxies with SBF measurements within

Send offprint requests to: S. Mei, e-mail: `simona.mei@ias.fr`

⋆ Based on observations performed at the European Southern Observatory, Paranal, Chile ESO program N° 66.A-0361.

Table 1. General properties of NGC 564 and NGC 7619, from the web archive Simbad (`http://simbad.u-strasbg.fr`) and the NASA/IPAC Extragalactic Database (NED) (`http://nedwww.ipac.caltech.edu/`).

Name	RA	DEC	Type	m_V^1	$V-I^1$	$cz_{\rm LG}^2$	$cz_{\rm CMB}^2$	$V_{\rm CMB}^{\rm pec2}$
	(2000)	(2000)		mag	mag	km s^{-1}	km s^{-1}	km s^{-1}
NGC 564	01 27 48.31	−01 52 47.68	E	13.01	1.2	5843	5037	−52
NGC 7619	23 20 14.68	+08 12 23.3	E	11.90	1.23	3758	3519	−256

[1] Prugniel & Heraudeau (1998), Poulain & Nieto (1994).
[2] Kelson et al. (2000) and references therein, Giovanelli (1998), Dale (1999).

Table 2. Read–out Noise and Gain for the four ports of FORS1 on VLT UT1.

Port	FORS1 Ron (e^-)	Gain (e^-/ADU)
A	5.01 ± 0.16	1.48 ± 0.04
B	5.42 ± 0.17	1.78 ± 0.05
C	5.18 ± 0.16	1.56 ± 0.04
D	5.03 ± 0.16	1.63 ± 0.05

1200 km s^{-1}. The Cepheid distances were part of a larger dataset used by HSTKP. The two calibrations are consistent within the errors.

Alternatively, theoretical calibrations have been obtained starting from synthesis models of the galaxy stellar population (Ajhar et al. 2001; Liu et al. 2000; Blakeslee et al. 2001). From Ajhar et al. (2001) the zero points of these calibrations provide an average value of the Hubble constant (H_0 = 77 ± 7 km s^{-1}/Mpc) that is in good agreement with the observational results.

With HST and 8-m class telescopes SBF measurements have been extended beyond the local universe (cz < 4000 km s^{-1}). While the survey by Tonry et al. (2001) was limited to galaxies with cz < 4000 km s^{-1}, using HST observations it has been possible to determine distances for more distant galaxies (Thomsen et al. 1997; Lauer et al. 1998; Pahre et al. 1999; Jensen et al. 2001; Liu et al. 2001; Ajhar et al. 2001), up to approximately 10 000 km s^{-1}.

In this paper we extend our ground-based I-band SBF measurements to beyond ≈5000 km s^{-1}. Advantages and disadvantages of I– versus K-band ground based SBF observations were discussed using theoretical simulations in Mei et al. (2001). Deep I–band SBF observations were obtained for two galaxies: NGC 564, in Abell 194, at $cz \approx 5800$ km s^{-1}, and NGC 7619 in the Pegasus cluster at $cz \approx 3700$ km s^{-1}. Both Abell 194 and Pegasus are fiducial clusters in the derivation of observational templates for the Tully–Fisher (TF) and Fundamental Plane (FP) relations (see for example Mould et al. 1991, 1993; Jorgensen et al. 1996; Giovanelli et al. 1998; Scodeggio et al. 1998; Dale et al. 1999; Hudson et al. 2001), while Abell 194 is also part of the sample of clusters studied by Lauer & Postman (1992, 1994). Although distance estimates obtained with the TF and FP relations are comparatively less accurate than those obtained with the SBF method, they are relatively easier to obtain, even for objects located at larger distances than those sampled so far by SBF observations. Therefore the most complete and farthest reaching mappings of the local universe currently make use of TF- and FP-based distances, and they will likely do so in the near future. One of the main motivations behind the selection of targets for this work was the possibility of providing a bridge between SBF distance estimates and TF or FP results, as this is the most direct way to improve the accuracy of the calibration for the latter relations, and consequently that of all distance estimates based on these relations. This effort extends to larger distances the matching of SBF and FP distance scales recently presented by Blakeslee et al. (2002).

In Sect. 2 we describe our observations, and the SBF analysis. The H_0 measurements and a summary of this analysis are presented in Sects. 3 and 4.

2. Surface brightness fluctuation analysis

2.1. Observations

NGC 564 and NGC 7619 were observed in service mode at the Very Large Telescope unit UT1 (Antu) at the European Southern Observatory in Paranal, Chile, using the FORS1 (FOcal Reducer and low dispersion Spectrograph) imaging camera with a 2048 × 2048 pixel Tektronix CCD. The properties of these galaxies are summarised in Table 1.

The FORS1 high gain, standard resolution mode was used, with a pixel scale 0.2″/pixel and field of view 6.8′ × 6.8′. The detector had four ports with different read out noise and gain. We show the gains for the different ports in Table 2. The dark current is negligible (<2e^-/pixel/hour at nominal operating temperature).

I–band and V–band data were obtained, to have an accurate $V-I$ colour to input into the Tonry et al. (2000) calibration of I–band SBF fluctuations. For NGC 564, the nights of observation were on 5 October, 3 November, 2, 19, 22 December 2000, and 1, 18 and 21 January 2001 for the I–band and on 19 August 2001 for the V–band. The raw data were 293 galaxy exposures each of ≈65 s in the I–band and 5 galaxy exposures each of 100 s in the V–band. The total observation time was 5.3 hrs in the I–band and 500 s in the V–band. For NGC 7619, the nights of observation were on 5 October 2000 for the I–band and the 3 November 2000 for the V–band. The raw data were 55 galaxy exposures each of ≈150 s, and 4 exposures of 60 s in the I–band, and 5 galaxy exposures each of 100 s in the V–band. The total observation time was 2.4 hrs in the I–band and 500 s in the V–band. A summary of observations is in Table 3.

The seeing was ≈0.8″ *FWHM* on the nights of observations. Data observed on different nights were calibrated to one photometric night observations for each galaxy in each band, by the use of reference stars in the images. In the case of NGC 7619, some of the images in I–band were not photometric

Table 3. Observations.

Galaxy	Band	Date	Frames	Exp. Time (s)
NGC 7619	*V*	3 Nov. 00	5	100
	I	5 Oct. 00	4	60
	I	5 Oct. 00	55	150
NGC 564	*V*	19 Aug. 01	5	100
	I	3 Nov. 00	81	65
	I	2 Dec. 00	53	65
	I	19 Dec. 00	41	65
	I	22 Dec. 00	41	65
	I	18 Jan. 01	41	65
	I	21 Jan. 01	36	65

and the final added image has been calibrated on a combination of photometric images.

All observations were obtained in VLT Service Mode. Bias corrected, flat-fielded, and trimmed frames were delivered by ESO and used by us without further processing. Further details about pipeline processed FORS science products and calibration can be found on the ESO Quality Control Web pages (`http://www.eso.org/qc/`).

The photometric zero-point and the extinction coefficient were extracted from observations of Landolt standards (Landolt 1992) and confirmed using the historical data available from the ESO Quality Control Web pages. The *I*–band filter in the FORS1 camera is a Bessel *I* filter, but all measurements were transformed into Kron-Cousins *I*–band magnitudes. In this magnitude scale, for NGC 564 the photometric zero-point is $m_1 = 26.59 \pm 0.02$ mag (m_1 is the zero magnitude which corresponds to a flux of 1 ADUs^{-1}) and the extinction coefficient 0.06±0.01 mag. The colour term correction in $(V-I)$ is -0.05 ± 0.03 mag. For NGC 7619, $m_1 = 26.60 \pm 0.02$ mag and the extinction coefficient 0.07 ± 0.01 mag.

In the *V*–band, the photometric zero-point was $m_1 = 27.53 \pm 0.02$ mag for NGC 564 and $m_1 = 27.45 \pm 0.02$ for NGC 7619, and the extinction coefficient was 0.11 ± 0.05 mag for NGC 564 and 0.12 ± 0.05 for NGC 7619. The colour term correction in $(V - I)$ is 0.03 ± 0.03 mag.

Bad pixels and cosmic rays were eliminated by a sigma clipping algorithm while combining the images using the IRAF[1] task IMCOMBINE. The images have been scaled in exposure time and median value. Sub-pixel registration was not used to avoid the introducing correlated noise between the pixels in the images.

2.2. SBF Measurements

The data were analysed with a standard two–step SBF extraction technique, as detailed, for example, by Tonry & Schneider (1988). Firstly, a smooth galaxy profile was subtracted from the image. The smoothed image was derived by fitting galaxy isophotes to the original image with the IRAF task ISOPHOTE, once visible external sources were subtracted. To account for residual errors that can be due to the galaxy profile subtraction, the resulting image was then smoothed on a scale ten times the width of the PSF, once additional point sources were identified and subtracted using the software tool Sextractor (Bertin & Arnouts 1996), and subtracted from the original image.

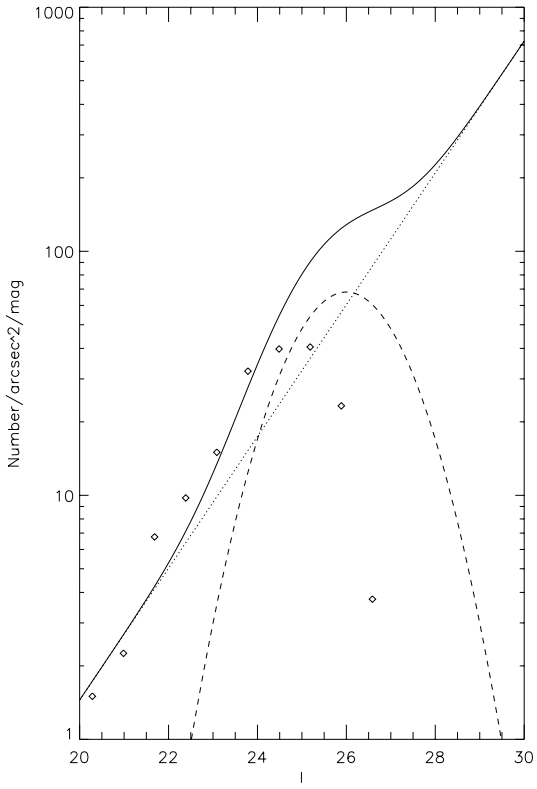

Fig. 1. We show NGC 564 external source luminosity function between 14″ and 23″ from the center of the galaxy. The solid line shows the sum of the globular cluster luminosity function plus the background galaxy luminosity function. The dashed line shows the fitted globular cluster luminosity function, the dotted line the background galaxy luminosity function.

Secondly, a new galaxy model was fit and subtracted to this difference image. In such way, the sky is also subtracted. In order to make the SBF fluctuations constant across the image, the difference image was finally divided by the square root of the new galaxy model.

This final image was then divided into different annuli, in each of which the power spectrum of the image fluctuations was calculated. The resulting power spectrum was azimuthally averaged, and normalised to the number of non-zero points in the annulus. The external point sources brighter than a magnitude $m_{\rm cut}$ where the completeness function of each annulus was greater than 50% were masked out.

Two components contribute to the total image power spectrum: the constant power spectrum due to the white noise, P_1, and the power spectrum of the fluctuations and point sources that are both convolved by the PSF in the spatial domain. In the Fourier domain these latter terms are given by a constant, P_0, multiplied by the power spectrum of the PSF:

$$E_{\rm gal} = P_0\, E_{\rm PSF} + P_1. \quad (1)$$

To compute P_0 and P_1, a robust linear least squares fit was made by minimising absolute deviation (Numerical Recipes,

[1] The Image Reduction and Analysis Facility (IRAF) is distributed by the National Optical Astronomy Observatories.

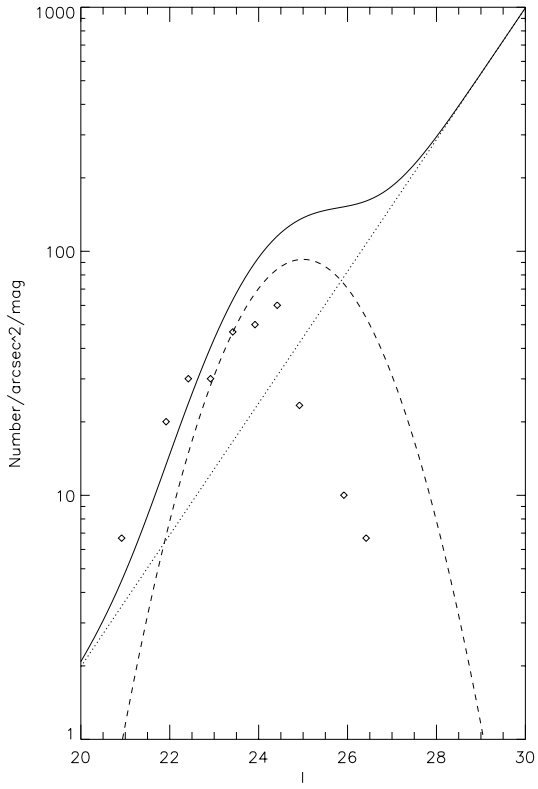

Fig. 2. We show NGC 7619 external source luminosity function between 20″ and 52″ from the center of the galaxy. The solid line shows the sum of the globular cluster luminosity function plus the background galaxy luminosity function. The dashed line shows the fitted globular cluster luminosity function, the dotted line the background galaxy luminosity function.

Press et al. 1992). As part of the fit, to calculate $E_{\rm PSF}$ a point spread function (PSF) profile was determined from the bright stars in the image and normalised to 1 ADUs^{-1}, following Tonry & Schneider (1988). This means that P_0 is directly the power that we wish to measure.

Low wave number (k) points were excluded from the fit (pixel scale greater than 20), because they are contaminated by the galaxy subtraction and subsequent smoothing.

As stated above, P_0 contains contributions from both SBF and unresolved point sources. The point source contribution $P_{\rm es}$ was estimated from the equations:

$$P_{\rm es} = \sigma^2_{\rm gc} + \sigma^2_{\rm bg} \tag{2}$$

following, i.e., Blakeslee & Tonry (1995); $\sigma^2_{\rm gc}$ is the contribution to the fluctuations given by globular clusters, $\sigma^2_{\rm bg}$ is the contribution by background galaxies. We adopted the following luminosity function for the globular clusters:

$$N_{\rm gc}(m) = \frac{N_{\rm ogc}}{\sqrt{2\pi}\sigma} {\rm e}^{\frac{-(m-m^{\rm gc}_{\rm peak})^2}{2\sigma^2}}. \tag{3}$$

We have assumed as initial $M^{\rm gc}_{{\rm peak}I} \approx -8.5$ and $\sigma = 1.35$ (Ferrarese et al. 2000b) with standard globular cluster colours (Gebhardt & Kissler-Patig 2000). For NGC 564, we have fitted to our detected globular cluster number counts an initial maximum likelihood $m^{\rm gc}_{{\rm peak}I} = 26$ and have assumed an initial galaxy distance modulus 34.4, from Kelson et al. (2000) and references therein. For NGC 7619, we have fitted to our detected globular cluster number counts an initial maximum likelihood $m^{\rm gc}_{{\rm peak}I} = 25$ and have assumed an initial galaxy distance modulus 33.5, from Dale et al. (1999). These initial values were iterated in the process of the SBF distance modulus calculation. The error on the external source contribution includes the uncertainties due to this iteration process. This last error has been calculated as the standard deviation of the estimation of the external source contribution for all the iterations, till stabilisation.

For the background galaxies, a power-law luminosity function was used:

$$N_{\rm bg}(m) = N_{\rm obg} 10^{\gamma m} \tag{4}$$

with $\gamma = 0.27$ (Smail et al. 1995). We kept as fixed parameters in the fit σ, γ, and iterated on $m^{\rm gc}_{\rm peak}$, as a function of the galaxy distance, while $N_{\rm ogc}$ and $N_{\rm obg}$ were estimated by fitting the composite luminosity function to the external sources extracted from the image in the range used for SBF measurements in each galaxy. Identified foreground stars were not included in the fit. From the estimated $N_{\rm ogc}$ and $N_{\rm obg}$ per pixel, $P_{\rm es}$ was calculated as the sum of:

$$\sigma^2_{\rm gc} = \tfrac{1}{2} N_{\rm ogc} 10^{0.8[m_1 - m^{\rm gc}_{\rm peak} + 0.4\sigma^2 \ln(10)]} \, erfc[\frac{m_{\rm cut} - m^{\rm gc}_{\rm peak} + 0.8\sigma^2 \ln(10)}{\sqrt{2}\sigma}] \tag{5}$$

and

$$\sigma^2_{\rm bg} = \frac{N_{\rm obg}}{(0.8-\gamma)\ln(10)} 10^{0.8(m_1 - m_{\rm cut}) + \gamma(m_{\rm cut})} \tag{6}$$

(Blakeslee & Tonry 1995), m_1 is the zero magnitude which corresponds to a flux of 1 ADUs^{-1}. The $P_{\rm es}$ were calculated over the luminosity function with this fitting procedure in each annulus, as in Sodemann & Thomsen (1995). To estimate $m_{\rm cut}$ we have calculated the completeness function of each annulus, adding artificial point sources to the original, galaxy subtracted image.

In the calculation of $P_{\rm es}$ the fact that $m_{\rm cut}$ corresponds to a completeness function of 50% has been taken in account, integrating the contribution on the source completeness function.

We show the respective external source luminosity functions of NGC 564 and NGC 7619 in Figs. 1 and 2.

The SBF amplitude is given by:

$$\overline{m}_I = -2.5\log(P_0 - P_{\rm es}) + m_1 - k_{\rm ext} sec(z) \tag{7}$$

where $k_{\rm ext}$ is the extinction coefficient and z the airmass for the observations. In the I–band, we measured $k_{\rm ext} = 0.06 \pm 0.01$ and $m_1 = 26.59 \pm 0.02$ for NGC 564, and $k_{\rm ext} = 0.07 \pm 0.01$ and $m_1 = 26.60 \pm 0.02$ for NGC 7619. The effective airmass for the nights that were used as photometric reference was $sec(z) = 1.2$ for NGC 564 and $sec(z) = 1.38$ for NGC 7619, as calculated with the IRAF task *setairmass* on all images from that night (3 November 2000) for NGC 564, and on the photometric images used as a reference for NGC 7619.

In the V–band, we measured $k_{\rm ext} = 0.11 \pm 0.01$ for NGC 564 and $k_{\rm ext} = 0.12 \pm 0.01$ for NGC 7619, and $m_1 = 27.53 \pm 0.02$ for NGC 564 and $m_1 = 27.45 \pm 0.02$ for NGC 7619. The effective airmass was $sec(z) = 1.2$ for NGC 564 and $sec(z) = 1.24$ for NGC 7619.

2.3. Results on NGC 564

The power spectrum fitting of NGC 564 is shown in Fig. 3. The results for each annulus are listed in Table 4. The SBF magnitudes were calculated from Eq. (7). The errors on SBF magnitudes for each annulus are the standard deviations among different wavelength cuts ($3 \lessapprox$ pixel scale $\lessapprox 20$). The errors due to external source residual contribution subtraction were added in quadrature to the fitting errors and to the errors due to the zero point magnitude and the $k_{\rm ext}$.

The SBF magnitudes $I_{o,k}$ were then corrected for galactic absorption assuming $E(B-V) = 0.038$, $A_I = 0.074$, and $A_V = 0.13$, from Schlegel et al. (1998), and a k–correction $k_I \approx 7\ z = 0.12$ for SBF was applied (Tonry et al. 1997; Liu et al. 2000), $\overline{I}_{o,k} = \overline{m}_I - A_I - k_I$. The total $A_I + k_I$ was equal to 0.19 mag.

The galaxy colour in each annulus is shown in Table 4. The error on each colour measurement was 0.03 mag. The colours that are shown in the table have been corrected for extinction. The adopted $A_I - A_V$ correction amounts to 0.056 mag. For the calculation of the galaxy colours the k–correction is $k_I = 1\ z$ and $k_V = 1.9\ z$.

From the Tonry et al. (2000) calibration:

$$\overline{M}_I = (-1.74 \pm 0.08) + (4.5 \pm 0.25)[(V-I)_0 - 1.15], \quad (8)$$

we derive the $\overline{M}_I$ shown in Table 4. The error on each value of $\overline{M}_I$ is $\sigma_{\overline{M}_I} = 0.18$. We did not add here the systematic uncertainty due to Cepheid calibration (Ferrarese et al. 2000a; Freedman et al. 2001) (see below).

From the calibration from Ferrarese et al. (2000a), revised to the Freedman et al. (2001) Cepheid distances (as from Ajhar et al. 2001):

$$\overline{M}_I = (-1.73 \pm 0.09) + (4.5 \pm 0.25)[(V-I)_0 - 1.15] \quad (9)$$

we would have obtained a difference in SBF absolute magnitude of 0.01 mag and the same statistical errors.

A systematic uncertainty from the Cepheid calibration amounting to 0.16 mag has to be added to both calibration zero points.

In each annulus we derive an estimated distance modulus $\overline{I}_{o,k} - \overline{M}_I$. A mean distance modulus was determined as the mean of the values in the considered annuli. The error is given by the standard deviation of those values, around the mean, divided by the square root of the number of considered values.

The final distance modulus is $(\overline{I}_{o,k} - \overline{M}_I) = 34.39 \pm 0.18$ and the galaxy distance 76 ± 6 Mpc. If we use the SBF calibration by Ferrarese et al. (2000a), we obtain: $(\overline{I}_{o,k} - \overline{M}_I) = 34.38 \pm 0.18$ and the galaxy distance 75 ± 6 Mpc.

To the statistical error has to be added a systematic uncertainty due to the Cepheid calibration that amounts to 6 Mpc.

2.4. Results on NGC 7619

The power spectrum fitting of NGC 7619 is shown in Fig. 4. The results for each annulus are listed in Table 5. As for NGC 564, the errors on SBF magnitudes for each annulus are the standard deviations among different wavelength cuts. The errors due to external source residual contribution subtraction were added in quadrature to the fitting errors and to the errors due to the zero point magnitude and the $k_{\rm ext}$.

The SBF magnitudes $I_{o,k}$ were then corrected for galactic absorption assuming $E(B-V) = 0.079$, $A_I = 0.153$, and $A_V = 0.261$, from Schlegel et al. (1998), and a k–correction $k_I \approx 7\ z = 0.08$ was applied (Tonry et al. 1997; Liu et al. 2000), $\overline{I}_{o,k} = \overline{m}_I - A_I - k_I$. The total $A_I + k_I$ was equal to 0.23 mag.

The galaxy colour in each annulus is shown in Table 5. The error on each measurement is equal to 0.03 mag. The colours that are shown in the table have been corrected for extinction. The adopted $A_I - A_V$ correction amounts to 0.11 mag.

From the Tonry et al. (2000) calibration we derive the $\overline{M}_I$ shown in Table 5. The error on each value of $\overline{M}_I$ is $\sigma_{\overline{M}_I} = 0.18$. As for NGC 564 with the Ferrarese et al. (2000a) calibration, we would have obtained a difference in SBF absolute magnitude of 0.01 mag and the same statistical errors.

Again, a systematic uncertainty from the Cepheid calibration amounting to 0.16 mag has to be added to both calibration zero points.

In each annulus we derive an estimated distance modulus $\overline{I}_{o,k} - \overline{M}_I$. A mean distance modulus was determined as the mean of the values in the considered annuli. The error is given by the standard deviation of those values, around the mean, divided by the square root of the number of considered values.

The final distance modulus is $(\overline{I}_{o,k} - \overline{M}_I) = 33.64 \pm 0.16$ and the galaxy distance 54 ± 4 Mpc. This value is compatible with Tonry et al. (2001) measurements ($\overline{M}_I = 33.62 \pm 0.31$).

3. H_0 measurement

The value for H_0 is derived from our distance measurements and the redshifts of the respective clusters of the galaxies. The cluster redshift and Tully-Fisher peculiar velocity were used.

For NGC 564 the recession velocity of the cluster A194 is $cz_{\rm CMB} = 5253 \pm 222$ km s^{-1} from Dale et al. (1999), and we derive the value of $H_0 = 70 \pm 7 \pm 6$ km s^{-1}/Mpc, where the second error is the systematic uncertainty due to the Cepheid calibration. For NGC 7619, in the Pegasus cluster, the cluster redshift is 3635 ± 221 km s^{-1} from Giovanelli et al. (1998), and we derive $H_0 = 68 \pm 6 \pm 6$ km s^{-1}/Mpc. When the Ferrarese et al. (2000a) calibration is used, we obtain the same values for H_0.

We have also measured the distance of IC 4296 from previous VLT measurements (Mei et al. 2000). From that measurement (49 ± 4 Mpc), and the flow corrected galaxy recession velocity $cz = 3341 \pm 552$ km s^{-1} (Ferrarese et al. 2000b), $H_0 = 68 \pm 10 \pm 6$ km s^{-1}/Mpc.

From our three galaxy sample, we obtain: $H_0 = 68 \pm 5 \pm 6$ km s^{-1}/Mpc.

Our errors are comparable the *Hubble Space Telescope Key Project on the Extragalactic Scale*. We can then measure the Hubble constant from the Ferrarese et al. (2000a) SBF sample (Freedman et al. 2001, Table 10) and our VLT three galaxy sample, calibrated on the revised Ferrarese et al. (2000a) calibration (Ajhar et al. 2001; Freedman et al. 2001).

The two samples (Ferrarese et al. and our sample calibrated with the Ferrarese et al. calibration, that gives us the same results than the Tonry et al. calibration) are shown in

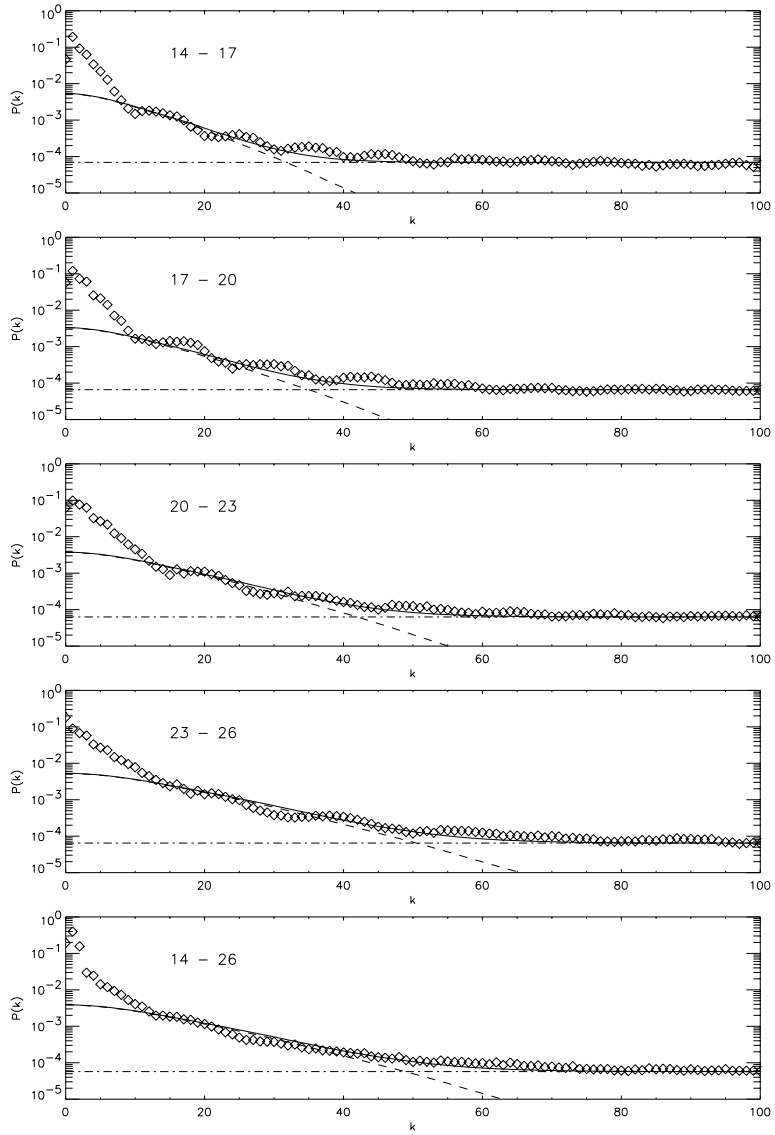

Fig. 3. NGC 564 SBF measurement. We show NGC 564 power spectrum as was fitted in five different annuli of width ≈3″ in the galaxy and on the full field up to 26″. The fit of the power spectrum is given by the solid line, the PSF power spectrum by the dashed line and the dashed-dotted line is the fitted constant white noise spectrum.

Table 4. SBF measurements for various annuli of NGC 564.

Annulus (″)	P_0	σ_{P_0}	$P_{\rm es}$	$\sigma_{P_{\rm es}}$	$(P_0 - P_{\rm es})/P_1$	$(V-I)_{\rm o}$	$\overline{M}_I$	$\overline{I}_{o,k}$	$\sigma_{\overline{I}_{o,k}}$	$\overline{I}_{o,k} - \overline{M}_I$	$\sigma_{(\overline{I}_{o,k}-\overline{M}_I)}$
14–17	0.0071	0.001	0.003	0.001	68	1.20	−1.52	32.4	0.5	33.92	0.5
17–20	0.0043	0.001	0.0015	0.0005	46	1.20	−1.52	32.8	0.4	34.32	0.4
20–23	0.0034	0.0004	0.0015	0.0005	32	1.21	−1.47	33.2	0.3	34.67	0.4
23–26	0.0040	0.0005	0.0015	0.0005	42	1.22	−1.43	32.9	0.3	34.33	0.4
14–26	0.0032	0.0002	0.0015	0.0005	28	1.20	−1.52	33.2	0.3	34.72	0.4
Mean All	–	–	–	–	–	–	–	–	–	34.39	0.18

Table 6, where the statistical errors on H_0 are given. IC 4296 is present in both Ferrarese and our sample. From the two combined samples we obtain $H_0 = 71 \pm 4 \pm 6$ km s^{-1}/Mpc. The first error is statistical, the second one is the systematic uncertainty due to the Cepheid calibration (Freedman et al. 2001). Our results are comparable with other I–band and K–band SBF measurements, and, increasing the I–band SBF sample beyond 3000 km s^{-1}, we have reduced the statistical error on I–band SBF H_0 measurements from Freedman et al. (2001) from 5 to 4 km s^{-1}/Mpc (their measurement is in fact: $H_0 = 70 \pm 5 \pm 6$ km s^{-1}/Mpc).

If we combine only galaxies beyond 4000 km s^{-1} from the two samples, we obtain $H_0 = 72 \pm 6 \pm 6$ km s^{-1}/Mpc.

There have been other two recent measurements of H_0 with I–band SBF, one from Tonry et al. (2001) with a sample of ≈300 ellipticals out to ≈3000 km s^{-1}, and their

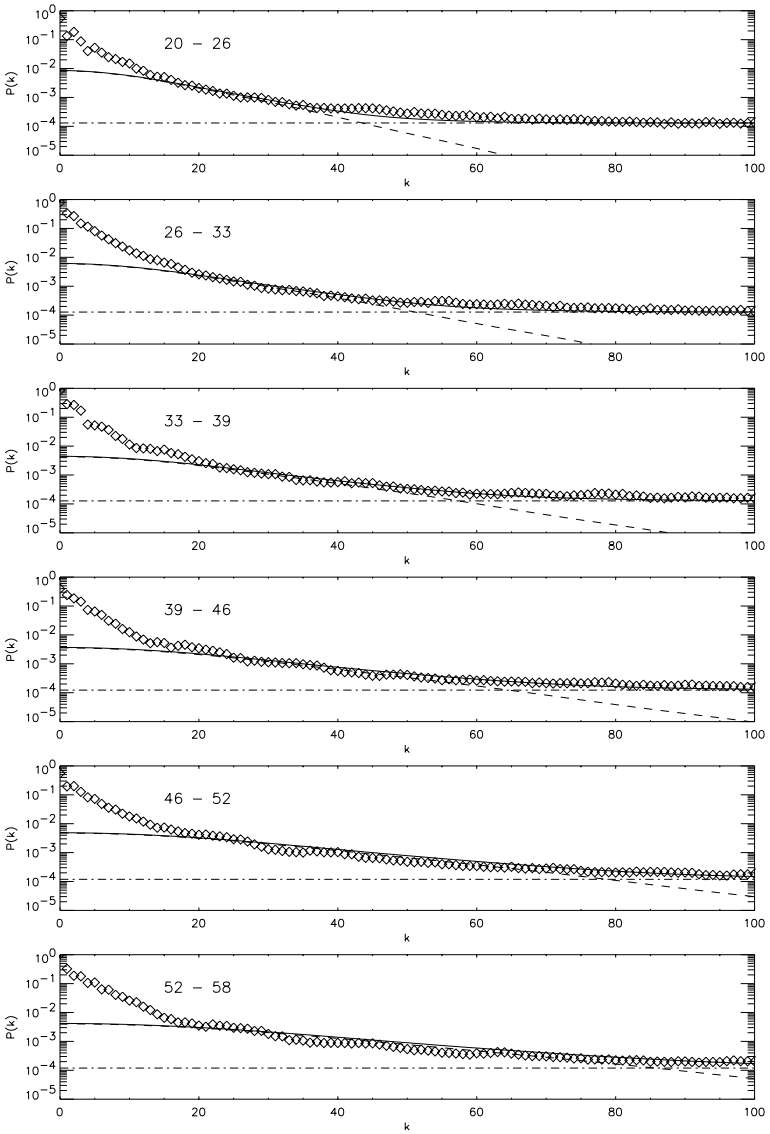

Fig. 4. NGC 7619 SBF measurement. We show NGC 7619 power spectrum as was fitted in six different annuli of width ≈6″. The fit of the power spectrum is given by the solid line, the PSF power spectrum by the dashed line and the dashed-dotted line is the fitted constant white noise spectrum.

Table 5. SBF measurements for various annuli of NGC 7619.

Annulus (″)	P_0	σ_{P_0}	$P_{\rm es}$	$\sigma_{P_{\rm es}}$	$(P_0 - P_{\rm es})/P_1$	$(V-I)_{\rm o}$	$\overline{M}_I$	$\overline{I}_{o,k}$	$\sigma_{\overline{I}_{o,k}}$	$\overline{I}_{o,k} - \overline{M}_I$	$\sigma_{(\overline{I}_{o,k}-\overline{M}_I)}$
20–26	0.014	0.001	0.01	0.01	30	1.23	−1.38	32.04	0.4	33.42	0.4
26–33	0.008	0.003	0.005	0.001	23	1.22	−1.43	32.16	0.4	33.58	0.4
33–39	0.005	0.001	0.002	0.001	23	1.21	−1.47	32.34	0.4	33.81	0.4
39–46	0.004	0.001	0.001	0.001	23	1.21	−1.47	32.26	0.3	33.73	0.4
46–52	0.005	0.001	0.0009	0.0005	34	1.21	−1.47	32.07	0.3	33.54	0.4
52–58	0.004	0.001	0.0009	0.0005	27	1.23	−1.38	32.39	0.3	33.77	0.4
Mean	–	–	–	–	–	–	–	–	–	33.64	0.16

cosmic flow reconstruction ($H_0 = 77 \pm 4 \pm 7$ km s^{-1}/Mpc), and another one from Blakeslee et al. (2001) from the comparison of part of the Tonry sample (≈160 ellipticals) with Fundamental Plane distances and IRAS density measurements ($H_0 = 73 \pm 4 \pm 7$ km s^{-1}/Mpc).

With *K*–band SBF measurements by NICMOS with HST, Jensen et al. (2001) have obtained $H_0 = 72 \pm 2.3 \pm 6$ km s^{-1}/Mpc, obtaining for the first time in H_0 measurements by SBF a statistical error comparable to the supernovae Type Ia one (2 km s^{-1}/Mpc, Freedman et al. 2001). Their sample includes a dozen of galaxies with distances beyond 4000 km s^{-1}. Liu & Graham (2001) from Keck *K*–band SBF plus HST *I*–band measurements have measured $H_0 = 71 \pm 8$ km s^{-1}/Mpc.

All these measurements are compatible within the errors.

Table 6. SBF measurements of H_0.

Sample	Galaxy	$V_{\rm itflow}$	H_0
		(km s^{-1})	(km s^{-1}/Mpc)
Ferrarese et al. (2000a)	NGC 4881[1]	7441	72.7 ±18.7
	NGC 4373[2]	3118	85.9 ± 17.2
	NGC 0708[3]	4831	70.8 ± 8.6
	NGC 5193[3]	3468	67.3 ± 12.4
	IC 4296[3]	3341	60.2 ± 11.2
	NGC 7014[3]	5041	75.2 ± 7.2
Mei et al. (2000)	IC 4296	3341	67 ± 10
This work	NGC 564	5208	70 ± 7
	NGC 7619	3571	68 ± 6

[1] Thomsen et al. (1997).

[2] Pahre et al. (1999).

[3] Lauer et al. (1998).

4. Summary and conclusions

We have measured the Hubble constant H_0 in NGC 564 at $cz \approx 5800$ km s^{-1} and in NGC 7619 at $cz \approx 3700$ km s^{-1} with deep I–band SBF distance measurements at the ESO Very Large Telescope (VLT). We obtain $H_0 = 70 \pm 7 \pm 6$ km s^{-1}/Mpc for NGC 564 and $H_0 = 68 \pm 6 \pm 6$ for NGC 7619. The actual SBF sample used for the measurement of H_0 in the Hubble Space Telescope Key Project on the Extragalactic Distance Scale (Freedman et al. 2001) amounts to six galaxies.

When we combine the measurements from this work with our previous VLT I–band SBF distance measurement in IC 4296 (Mei et al. 2000), we obtain: $H_0 = 68 \pm 5 \pm 6$ km s^{-1}/Mpc. When we add the Freedman et al. (2001) SBF sample and calibrate our sample with the revised Ferrarese et al. (2000a) calibration (Ajhar et al. 2001; Freedman et al. 2001), we obtain $H_0 = 71 \pm 4 \pm 6$ km s^{-1}/Mpc. If we combine only galaxies beyond 4000 km s^{-1} from the two samples, we obtain $H_0 = 72 \pm 6 \pm 6$ km s^{-1}/Mpc).

Our results are comparable with other I–band and K–band SBF measurements. More importantly we have increased the number of galaxies in the I–band sample with redshifts larger than 3000 km s^{-1}, and thereby reduced the statistical error on I–band SBF H_0 measurements from the Freedman et al. (2001) value of 5 km s^{-1}/Mpc to 4 km s^{-1}/Mpc (their measurement is in fact: $H_0 = 70 \pm 5 \pm 6$ km s^{-1}/Mpc).

Few galaxies beyond the Fornax cluster have I–band SBF measurements and only five (included NGC 564 from this paper) have distances beyond 4000 km s^{-1}. This lack of distant galaxies is responsible for the fact that the statistical error on H_0 obtained with SBF measurements is still comparable to the systematic uncertainty due to the Cepheid calibration, which is not the case for SNIa and TF methods (with a statistical error of, respectively, 2 km s^{-1}/Mpc and 3 km s^{-1}/Mpc, Freedman et al. 2001). SBF being one of the most precise distance indicators, it is important to further reduce the statistical uncertainties. To achieve this, additional SBF measurements beyond 4000 km s^{-1} are needed.

Acknowledgements. S. Mei acknowledges support from the European Space Agency External Fellowship programme. We thank our referee, John Blakeslee for his comments useful for the improvement of this paper.

References

Ajhar, E. A., Tonry, J. L., Blakeslee, J. P., et al. 2001, ApJ, 559, 584
Ajhar, E. A., Lauer, T. R., Tonry, J. L., et al. 1997, AJ, 114, 626
Bertin, E., & Arnouts, S. 1996, A&AS, 117, 393
Blakeslee, J. P., Lucey, J. R., Tonry, J. L., et al. 2002, MNRAS, 330, 443
Blakeslee, J. P., Lucey, J. R., Barris, B. J., et al. 2001, MNRAS, 327, 1004
Blakeslee, J. P., Ajhar, E. A., & Tonry, J. L. 1999a, in Post-Hipparcos Cosmic Candles, ed. A. Heck, & F. Caputo (Boston: Kluwer), 181
Blakeslee, J. P., Davis, M., Tonry, J. L., et al. 1999b, ApJ, 527, L73
Blakeslee, J. P., & Tonry, J. L. 1995, ApJ, 442, 579
Colless, M., Saglia, R. P., Burstein, D., et al. 2001, MNRAS, 321, 277
Dale, D. A., Giovanelli, R., Haynes, M. P., et al. 1999, AJ, 118, 1489
Davis, M., Miller, A., & White, S. D. M. 1997, ApJ, 490, 63
Ferrarese, L., Mould, J. L., & Kennicutt, R. C. 2000a, ApJ, 529, 745
Ferrarese, L., Ford, H. C., Huchra, J., et al. 2000b, ApJS, 128, 431
Freedman, W. L., Madore, B. F., Gibson, B. K., et al. 2001, ApJ, 553, 47
Gebhardt, K., & Kissler-Patig, M. 2000, AJ, 118, 1526
Gibson, B. K., & Stetson, P. B. 2001, ApJ, 547, L103
Giovanelli, R., Haynes, M. P., Herter, T., et al. 1997, AJ, 113, 22
Giovanelli, R., Haynes, M. P., Salzer, J. J., et al. 1998, AJ, 116, 2632
Hanuschick, R., & Amico, P. 2000, Messenger, 99
Hjorth, J., & Tanvir, N. R. 1997, ApJ, 482, 68
Holtzman, J. A., Burrows, C. J., Casertano, S., et al. 1995, PASP, 107, 1065
Hudson, M. J., Lucey, J. R., Smith, R. J., et al. 2001, MNRAS, 327, 265
Jensen, J. B., Tonry, J. L., Thompson, R. I., et al. 2001, ApJ, 550, 503
Jensen, J. B., Tonry, J. L., & Luppino, G. A. 1999, ApJ, 510, 71
Jorgensen, I., Franx, M., & Kjaergaard, P. 1996, MNRAS, 280, 167
Kelson, D. D., Illingworth, G. D., Tonry, J. L., et al. 2000, ApJ, 529, 768
Landolt, A. U. 1992, AJ, 104, 340
Lauer, T. R., & Postman, M. 1992, ApJ, 400, L47
Lauer, T. R., & Postman, M. 1994, ApJ, 425, 418
Lauer, T. R., Tonry, J. L., Postman, M., et al. 1998, ApJ, 499, 577
Liu, M. C., & Graham, J. R. 2001, ApJ, 557, L31
Liu, M. C., Charlot, S., & Graham, G. R. 2000, ApJ, 543, 664
Mei, S., Silva, D. R., & Quinn, P. J. 2000, A&A, 361, 68
Mei, S., Quinn, P. J., & Silva, D. R. 2001, A&A, 371, 779
Mould, J. R., Han, M. S., Roth, J., et al. 1991, ApJ, 383, 467
Mould, J. R., Akeson, R. L., Bothun, G. D., et al. 1993, ApJ, 409, 14
Pahre, M. A., & Mould, J. R. 1994, ApJ, 433, 567
Pahre, M. A., Mould, J. R., Dressler, A., et al. 1999, ApJ, 515, 79
Press, W. H., et al. 1992, Numerical Recipes (Cambridge University Press, New York)
Prugniel, P., & Heraudeau, P. 1998, A&AS, 128, 299
Jha, S., Garnavich, P. M., Kirshner, R. P., et al. 1999, ApJS, 125, 73
Scodeggio, M., Giovanello, R., & Haynes, M. 1998, AJ, 116, 2728
Smail, I., Hogg, D. W., Yan, L., et al. 1995, ApJ, 449, L105
Sodemann, M., & Thomsen, B. 1995, AJ, 110, 179
Sodemann, M., & Thomsen, B. 1996, AJ, 111, 208
Suntzeff, N. B., Phillips, M. M., Covarrubias, R., et al. 1999, AJ, 117, 1775
Thomsen, B., Baum, W. A., Hammergren, M., et al. 1997, ApJ, 483, L37
Tonry, J. L., & Schneider, D. P. 1988, AJ, 96, 807
Tonry, J. L., Blakeslee, J. P., Ajhar, E. A., et al. 1997, ApJ, 475, 399
Tonry, J. L., Blakeslee, J. P., Ajhar, E. A., et al. 2000, ApJ, 530, 625
Tonry, J. L., Dressler, A., Blakeslee, J. P., et al. 2001, ApJ, 546, 681